

THE HAYSTACK AND HAYSTACK AUXILIARY RADARS AND THEIR
ROLE IN ORBITAL DEBRIS ENVIRONMENT CHARACTERIZATION

Dr. John U. Beusch Dr. Antonio F. Pensa Dr. Brian W. Zuerndorfer

MIT Lincoln Laboratory 244 Wood Street Lexington, MA 02173 USA

ABSTRACT

MIT Lincoln Laboratory's Haystack Radar was selected to conduct a program of extensive measurements of the orbital debris environment. An additional capability, the Haystack Auxiliary Radar (HAX), has been developed. The orbital debris measurements completed to date on this program represent a significant portion of the hard data available on the aggregate number of small debris objects in orbit today.

A special purpose processing system was developed for the Haystack/HAX orbital debris measurement program. This system decides in real time which data to record and which to discard based on properties of the data itself.

A main issue in debris characterization is radar calibration. This includes not only the absolute calibration at the peak of the radar beam but also precise mapping of the two dimensional sum and difference beams. Extensive calibration is important because approximate orbital parameters of each debris object are needed and can only be estimated on a single pass of the object through the beam. This requires that measurements be made across a major part of the beamwidth.

The accuracy of the Haystack orbital debris measurement results is explained and implications of the results are discussed. The capability of the HAX for orbital debris measurement is briefly described.

ACKNOWLEDGEMENTS

The authors would like to acknowledge the contributions of the many people involved in the orbital debris data collection effort with the Haystack Radar. Israel Kupiec developed the original idea for the effort and has been instrumental throughout. Tom Sangiolo and Tom Morgan have been key contributors throughout the program. Richard Abbott, Mike Gaposchkin, and Bob Miller were contributions to the radar calibration effort. Leo Nolan and Ed May, past and present system engineers at the radar, performed radar measurements between missions. Bob French, Hung Nguyen, Kevin Kelley, Jim Anderson, and Rich Brockelman developed software. Charlie Diorio and Judy Crouse reduced data at all hours of the day and night. Dave Pippin and Paul Lavoie planned and supervised mission operations. Chris Cullinane and Scott Wacker kept the data flowing between Millstone and Haystack for radar calibrations.

Finally, a special acknowledgement goes to all the men and women of the Haystack Radar under the leadership of Ray Landry. Literally everyone was impacted by this orbital debris effort, and we are grateful to them for their efforts and sacrifices of the past two years.

1. INTRODUCTION

MIT Lincoln Laboratory's X-Band Haystack Radar has been selected to conduct a program of extensive measurements of the orbital space debris environment. A companion Ku-Band radar known as the Haystack Auxiliary Radar (HAX) or Near Earth Assessment Radar (NEAR), recently implemented, will perform complementary measurements. The program was enabled by a Memorandum of Agreement between the United States Space Command and NASA which provides for NASA to receive 400 hours of debris data collection in FY 1990 from the Haystack Radar, 800 hours in FY 1991, 700 hours in FY 1992, and 800 hours each year for FY 1993 through FY 1997. The 1900 hours of Haystack Radar data for the first three years have been collected and the FY 1993 collection is currently underway. The Agreement also provides for 800 hours per year of data collection with HAX through FY 1997.

The objective of the Haystack and HAX data collection is to provide validation and parameter estimation for statistical models of the orbital debris population. Precise tracking and measurement of detailed properties of individual debris objects is not planned. In calibrating the radars it is especially important to avoid bias error; if all measurement errors are random in nature with zero mean their effects on the statistical models can be diminished by increasing the sample size, i.e. increasing the number of hours of debris data collection.

2. FEATURES OF SPACE OBJECTS

A particular piece of space debris could have a wide variety of shapes, sizes, material constitution, etc. These possibilities are described in numerous papers in the literature and in other papers at this conference. From the viewpoint of radar measurements a debris object must present a sufficiently large radar cross section (RCS) to be detected, at one or the other or in a combination of two polarizations. Required from the radar are well-calibrated estimates of the RCS which can be employed to estimate properties of the debris object such as mass and destruction capability upon the event of collision with a spacecraft, e.g. Space Station Freedom. Estimation of these properties from RCS data is outside the scope of this paper. Desired from the radar are estimates of the orbital parameters of the debris object.

A brief discussion of polarization may be helpful at this point. The Haystack Radar transmits an electromagnetic wave with right circular polarization and is instrumented to receive the energy reflected back from a space object. The electromagnetic wave containing this reflected energy can be decomposed into left circular polarization and right circular polarization, denoted as principal (PP) and opposite (OP) polarizations respectively. Thus the Haystack Radar has in its receiver both PP and OP channels.

In general, a piece of space debris or a spacecraft returns to the Haystack Radar signals in both the PP and OP channels. There are in orbit several metallic radar calibration spheres which possess, to a good approximation, the shape of a perfect sphere. A perfect sphere returns only PP signals to the Haystack Radar which represents a limitation in the calibration process. This limitation is discussed below and is a key point relative to the important issue of radar calibration. Heuristically, PP signals are returned from scattering features on an object that are "smooth" and OP signals are returned from internal corners which exhibit "double bounce" phenomena. This is a simplified explanation. If there were in orbit a perfect corner reflector oriented properly with respect to the radar line-of-sight, one could directly calibrate the OP channel and evaluate coupling between the OP and PP receive channels.

3. THE HAYSTACK RADAR

Figure 1 shows the Haystack Site in relation to other facilities which comprise the Millstone Hill Sensors. The Firepond Laser Radar is on the left, the Millstone Long Range Tracking Radar is on the right and the approximately spherical Haystack radome is in the center background. Also shown is a UHF tracking radar and atmospheric measurement facilities. The L-Band Millstone Radar is an important partner to Haystack in calibration tests since it provides precise orbital information on the radar calibration spheres.

Figure 2 shows a cut-away view of the Haystack Radome. The antenna is used for radio astronomy research in addition to its radar function. Different functions require different RF boxes. The radar box is shown being lifted into place in Figure 2. The Haystack antenna has a cassegrain feed, is 36 meters in diameter and is routinely employed up to 50 GHz for radio astronomy. It has a recently improved subreflector which permits limited operation up to 100 GHz. Thus, its performance at X-Band is very good. The one-way half-power beamwidth is 0.05 degrees; other key parameters of the radar are shown in Table I. In the literature the Haystack Radar is frequently referred to as the Long Range Imaging Radar (LRIR). All of the radar's digital processing systems were upgraded in the late

1980's with the new Processing and Control System (PACS). See Reference 1. The flexibility and high throughput of PACS are key elements that enable the radar, with fairly simple modification, to collect orbital debris data in a mode which is different from the normal wideband and narrowband tracking modes.

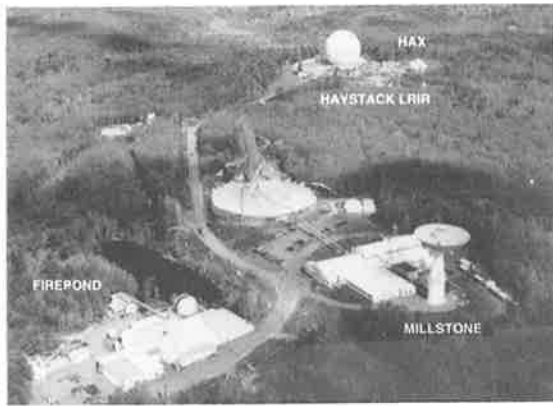


Figure 1. Millstone Hill sensors



Figure 2. Haystack antenna and radar box.

Table I

Center Frequency	10 GHz
Antenna Diameter	36m
Beam Width	0.05°
Peak Power	400 Kw
Pulse Repetition Frequency	30-1350 pps

The receiver microwave configuration is shown in Figure 3. A multimode horn illuminates the subreflector and receives the backscattered energy from the debris object. The monopulse receive networks combine signals to form the PP and OP sum and difference channels (beams). The OP azimuth and elevation difference channels are terminated and the sum and PP difference channels are formed. We will abbreviate the terms for these azimuth and elevation difference channels, denoted in the figure ΔAz_{pp} and ΔEl_{pp} , to ΔAz and ΔEl .

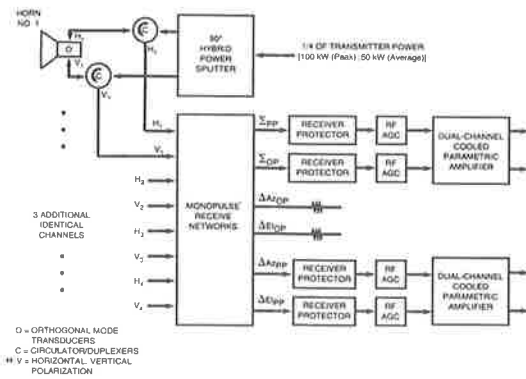


Figure 3. Haystack Radar receiver microwave configuration.

A brief discussion of the monopulse angle measurement process may be useful. *Monopulse* refers to the process of using multiple antenna beams on receive, which are offset in azimuth and elevation angle from the antenna boresite, to estimate the off-boresite angles of an object using a *single pulse*. The two symmetrically offset azimuth beams are subtracted (180° phase difference) to feed the ΔAz channel; similarly the elevation-offset beams feed the ΔEL channel. Angle estimates are formed by normalizing the signals in the difference channels by dividing by the signal in the PP sum channel.

The usual operating mode for the Haystack Radar (and most other tracking radars) is to track an object as near as possible to boresite, i.e. employ the signals in the difference channels to drive servos toward the boresite nulls in the difference beams. Operation for debris characterization is different. Antenna pointing is fixed, the debris object crosses the beams, and off-boresite angle estimates are made on every radar pulse received from the object as it crosses the beam. To make accurate off-boresite angle estimates, which are required to locate the object in the sum beam to estimate RCS orbital parameters, requires better calibration of the monopulse characteristics than had previously been required.

Each of the four channels in Figure 3 are followed by the components shown in Figure 4. For the antenna, and the RF and analog components of Figures 3 and 4, calibration is an issue. The Haystack Radar employs a digitally implemented single channel to I/Q conversion with inherent high stability so this portion of the system is not a driving factor in requiring frequent radar calibrations. The detection and recording systems implemented as a relatively minor modification to PACS are shown in Figure 5. Data on each pulse are directed to both the detection and recording buffers. A running non-coherent integration of the amplitude (sum channels) of 12 pulses is maintained in the detection buffer and when a threshold is crossed by this integrated signal, appropriate information in the recording buffer is recorded on tape. All data on 6 pulses preceding and following the threshold crossing are recorded. The threshold is set low enough that debris objects of the required RCS are seldom missed; however, frequent false alarms are recorded. False alarms due to noise are easy to filter out in subsequent data processing steps because their recorded information is different from that recorded for debris objects. The amplitudes, angle measurements, etc. on each pulse are not consistent with an object crossing the radar beams. The number of consecutive detections are also not consistent with an object that penetrates the sum beam.

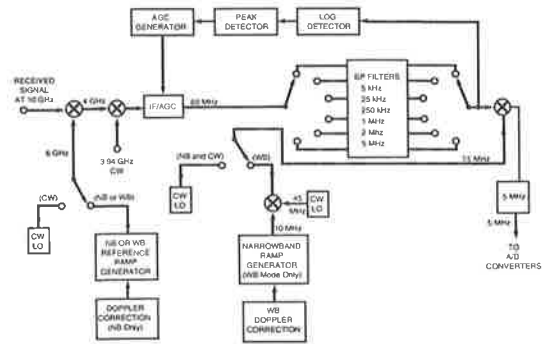


Figure 4. Receiver (One of the four channels).

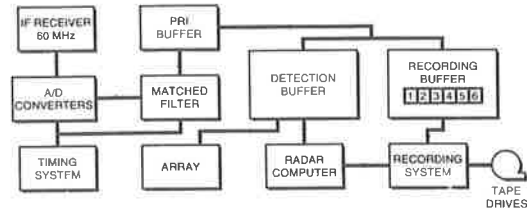


Figure 5. Detection and recording systems.

4. RADAR OPERATION FOR DEBRIS DATA COLLECTION AND CALIBRATION

Debris data collection is accomplished with the antenna in a fixed position: vertical (90° elevation), toward the south at 10° elevation, or in one of a few intermediate positions. Haystack is located at 41° north latitude. Figure 6 shows the orbital geometry and indicates that data from Haystack in the 10° elevation configuration comes from approximately the same volume as would come from a radar located at approximately 28° north latitude and pointing at 90° elevation.

The Haystack Radar transmits pulses of approximately 1 msec duration with a pulse repetition frequency of 40 Hz and bandwidth of 1 MHz. The system receives and processes any returns from objects as well as noise and records data when a threshold is crossed as previously discussed. Both this orbital debris data and all calibration data which includes precise measurements of the sum and difference beams of the antenna are provided to NASA for further processing and evaluation. From signal amplitude of each pulse on the four receiver channels, the PP and OP RCS's of a debris object can be estimated using the Σ_{pp} and Σ_{op} channel data adjusted by the sum beam antenna patterns based on the off-axis (Az and EL monopulse estimate) angle measurements. Object altitude and orbital inclination can be estimated from precise range measurements and less-precise off-axis angle estimates. Orbit eccentricity can usually not be estimated with good accuracy. Accuracy of estimates are discussed in Section 6.

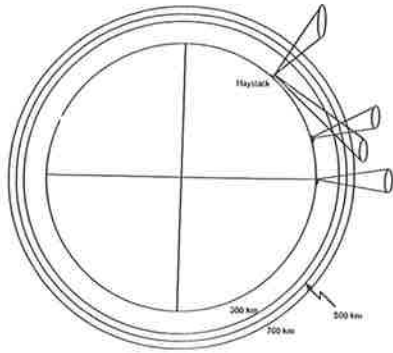


Figure 6. Haystack debris measurement geometry.

Calibration is required to ensure that the radar is setup properly prior to a debris collection mission. Calibration constants are initially and periodically (daily) determined with high accuracy. Also, system parameters are monitored to determine if adjustment or system maintenance is required. A mission has a duration of one, two or occasionally three weeks.

At the beginning of a mission the subreflector is positioned and read-outs of subreflector actuators is checked. During the mission alignment of the subreflector is monitored using tracks of satellites, SSC Numbers 7646, 16908, and 8820. These objects have very well-known orbits and are referred as metric satellites.

Five tests constitute the daily calibration activities and are used to maintain a calibration data base. They are the *noise, sensitivity, injection, monopulse, and channel phasing tests*. These tests are initialized within the first few hours of each mission and continue with measurements made once every 12 hours throughout the mission. Data collection intervals never exceed 10 hours without calibration. These daily activities are concerned with amplitude and phase variations of the receiver channels, which can occur over the course of a few days.

The *noise* test is performed by placing the antenna at 45° elevation and recording data on all four (Figure 3) receiver channels. This test augments the standard daily noise calibration tests. See Reference 2.

Fundamental to the remaining calibration procedures is the availability of calibration spheres in orbit. The Millstone Radar routinely tracks and maintains high-quality orbits on SSC Numbers 900, 902, 1361, 1512, 1520, and 5398. The orbital parameters are used in the Haystack calibration process. *Sensitivity* tests are performed by tracking a calibration sphere and recording Σ pp channel data. The recorded data are used to estimate radar sensitivity and monitor the Σ pp calibration constant.

Similarly, sensitivity tests on the Σ op channel should be performed by tracking orbiting objects with strong, stable, and known OP radar cross sections. However, no such objects are available. This short-coming is mitigated by making Σ op channel calibration measurements prior to data-collection missions, with the radar box on the ground. The OP/PP ratio is estimated by using a calibrated horn equipped with a polarizer, which illuminates the radar feed with both linear and circular polarization; Σ op/ Σ pp is recorded. The resulting measurement calibrates most of the system; the missing element is a small amount of depolarization caused by the dish antenna. By performing *injection* tests, i.e. monitoring the amplitude and phase of the four receiver channels using calibrated injection signals before and after the measurements, the state of the receiver is characterized in concert with the OP/PP ratio estimate. Given a radar OP/PP estimate with corresponding injection test data, subsequent OP channel radar cross section calibration constants are determined by simply monitoring OP/PP data from injection tests conducted during the data collection mission. As indicated, injection tests are repeated every 12 hours during the mission. The Σ op channel is then calibrated using the PP sensitivity results.

Calibration of the other two channels, Δ Az and Δ EL, like the Σ pp channel, is accomplished with observations of selected calibration spheres using monopulse and channel-phasing tests. *Monopulse* tests are an end-to-end monitor of monopulse processing. These tests are performed by tracking a calibration sphere using a spiral scan in which the antenna is driven in a spiral motion about the estimated position of the sphere; the sphere is tracked before and after each spiral. Data are recorded on all four receiver channels before, during and after each spiral and the reduced data are processed to calibrate the monopulse error gradient as discussed in Section 5.

Channel phasing monitors the phase of the two monopulse channels and the phase of each channel is adjusted if it deviates from 0°/180° relative to the Σ pp channel by more than 15°. Data to support channel phasing is recorded in conjunction with the monopulse tests as follows. Az-cut and EL-cut scans are included with the spiral scans in the monopulse tests. In an Az-cut scan, the antenna is driven so that the sphere passes through the beam in azimuth while remaining on boresite in elevation. In an EL-cut scan, the sphere passes through the beam in elevation while remaining on boresite in azimuth. Thus the signals on Δ Az/ Σ pp and Δ EL/ Σ pp are recorded separately and the phase at zero crossing for each is measured.

In addition to the daily calibration activities previously discussed, radar *metric monitoring* is performed during each mission, and serves to characterize radar pointing accuracy. During the first day, high elevation passes of metric reference satellites are tracked from as much of the pass as possible. Subsequent metric tracks during the mission monitor any systematic changes that may occur. Pointing accuracy is evaluated using Millstone's orbits.

5. CALIBRATION RESULTS

Some of the calibration tests result in occasional adjustment of radar parameters, e.g. phase adjustments. Others provide data used in subsequent debris data processing and in estimating the accuracy of the results. We discuss the latter category in this section.

Radar cross section and noise power in the Σ pp channel are monitored as part of the PP radar cross section calibration. Both parameters are determined from tracks of calibration spheres. The source of data for PP radar cross section are the sensitivity tests. In these tests, calibration spheres are tracked using all waveforms. Special attention is given to the 1 msec, CW waveform of debris data collection. The radar cross section of a sphere is determined from the output of peak range and Doppler cells in the Σ pp channel. Noise estimates are made using PP range and Doppler cells that are free of sphere returns, and are in units of equivalent radar cross section (dBsm). Signal-to-noise is formed from the ratio of radar cross section to noise power.

Figure 7 shows the error between measured Σ pp channel radar cross section and actual calibration sphere radar cross section. The figure shows typical PP radar cross section estimates with less than 0.5 dB rms error. Simultaneously, the Σ pp channel signal-to-noise ratio is typically measured to be 55.0 dB. This value corresponds to a 256 usec pulse width, 1000 km range, 56 dBw transmit power, and 0 dBsm target.

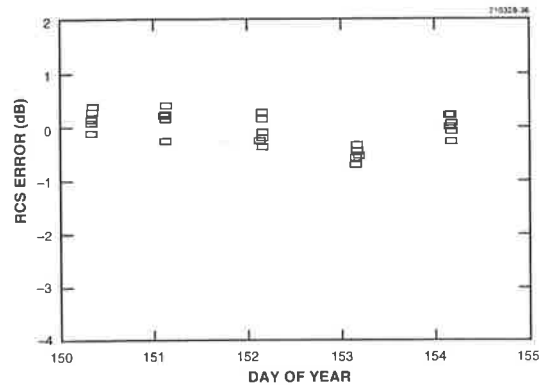


Figure 7. Σ pp Channel radar cross section error.

As previously discussed, the OP/PP amplitude ratio is estimated prior to a mission from measurements on the radar box. As an example, OP/PP ratio estimates were made with the radar box on the ground in February 1992. At that time, the radar OP/PP ratio was estimated at approximately -1.1 dB from measurements using the calibration horn and polarizer. Injection tests performed on the following day showed an OP/PP ratio of approximately -1.3 dB. Recall that injection test data are recorded for calibrated signals injected into the RF combiner. Consequently, the -1.3 dB OP/PP injection test result is a factor in the -1.1 radar OP/PP estimate, and there is a 0.2 dB OP/PP gain through the combiner and the feed. This gain was used to calculate the Σ op channel radar cross section calibration constant for the May 1992 mission. Figure 8 shows OP/PP amplitude ratio as a function of day number for the injection tests of the May mission. The average OP/PP ratio was -0.4 dB. By combining this with the 0.2 dB OP/PP (feed and combiner) gain determined in February, the estimated radar OP/PP ratio for the May mission is -0.2 dB.

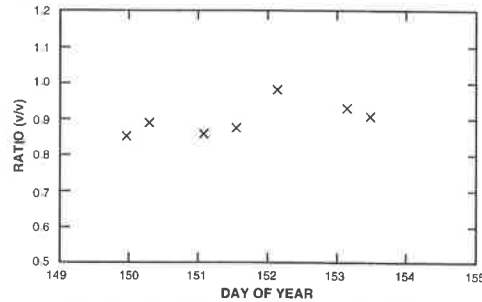


Figure 8. Injection test Σ op/ Σ pp amplitude data.

In the monopulse tests, Σ pp, Δ Az, and Δ EL data are recorded during each spiral. With precise knowledge of target position, voltage ratios (i.e., Δ Az/ Σ pp and Δ EL/ Σ pp) are calculated as functions of offset between antenna pointing angle and object position. Two-dimensional linear fits are made to these voltage ratio data, where the slopes of these fits represent the monopulse slopes.

The critical factors in the monopulse estimation process are (1) accurate estimation of object position and (2) regression analyses of monopulse slopes.

To support the space surveillance network, Millstone tracks satellites SSC Nos. 900, 902, 1361, 1512, 1520, and 5398. Table II summarizes the large number of Millstone tracks for the four of these objects used for radar calibration during a typical mission.

Table II
Number of Millstone tracks taken per satellite during the October 1991 mission

Mission	Satellite	# of Tracks
October 1991	1361	25
	5398	18
	1512	16
	1520	19

For the Haystack monopulse calibration, the angle accuracies of the orbital estimates are the important quantities. For 1361, which has been used for about 65% of the monopulse calibration to date, the orbit accuracy as measured in terms of the angles is better than a millidegree. For 1512, the next most used sphere for monopulse calibration (12%), the accuracy measure is also generally better than a millidegree. For 1520 (used about 10% of the time) the orbit quality is not quite as good—with a mean error of the orbit comparisons of a millidegree but rms values of the orbit differences up to 10 millidegrees. For 5398, the quality of the orbits, although sufficient for the purpose of the monopulse calibration, has been variable. The cases of poorer orbits have been due to the limited amount of tracking data available. The monopulse calibration has not relied heavily of 5398 (it is used about 5% of the time), and in the final reporting of the slopes, the best orbits are used.

Monopulse processing and data editing schemes for calibration are discussed in Reference 2. Figure 9 shows binned raw data for elevation during a spiral scan, and Figure 10 shows the surface after editing. With the data edited, calibration parameters are estimated using an interactive, two-parameter linear model; a 3 σ screening process is included to further eliminate bad data points.

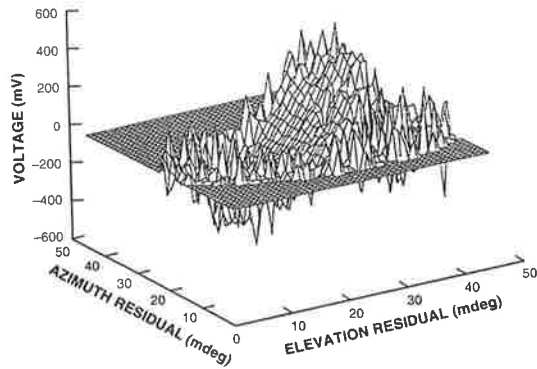


Figure 9. Spiral scan elevation data for SSC No. 1361.

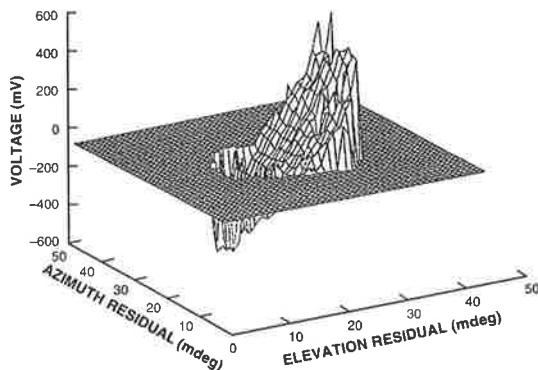


Figure 10. Edited spiral scan data.

Figure 11 shows monopulse gradient as a function of day number and object number for the May 1992 mission. The monopulse error gradient, or simply the *monopulse gradient*, is the reciprocal of the monopulse slope and represents the factor used to convert a monopulse value into (offset) angle. The monopulse output has the units of volts/volt, while angle is in degrees. The figures show typical monopulse gradient stability throughout a mission. In general, data from daily calibration tests show that monopulse slopes vary between 5% and 10% during a mission.

Injection tests are used to monitor the ΔAz , ΔEL , and Σop receiver channels, relative to Σpp . Receiver channel variability is a source of monopulse and radar cross section calibration variability. Injection tests are useful because they can monitor channel variability and be performed as needed throughout a mission; they do not require calibrated satellite tracks.

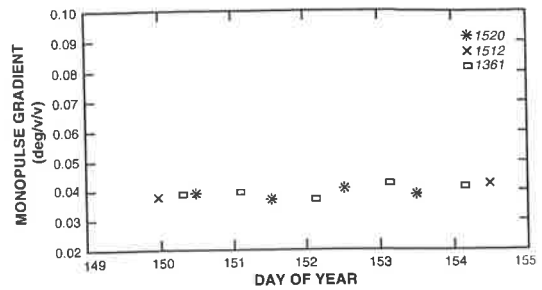


Figure 11. Elevation monopulse gradients.

In the injection tests, receiver data are recorded for calibrated signals injected into the RF combiner. In Figure 12 the amplitude ratios $\Delta Az/\Sigma pp$ and $\Delta EL/\Sigma pp$ are plotted as a function of day number for a typical mission. The figure shows roughly equal $\Delta Az/PP$ and $\Delta EL/PP$ ratios of 1.0 v/v. Using results from an earlier mission, injection test results yield estimated elevation monopulse gradients of 0.041. This estimated gradient is in agreement with the measured gradient shown in Figure 11.

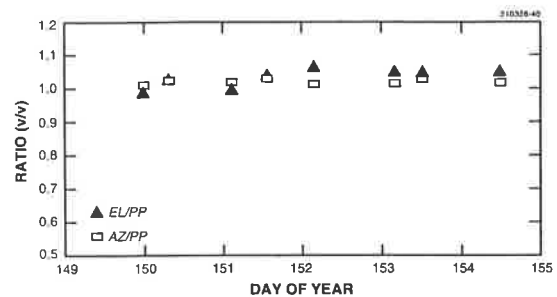


Figure 12. Injection test amplitude ratios.

6. ACCURACY AND RELIABILITY OF ORBITAL DEBRIS MEASUREMENTS

The reliability of debris object detection is expected to be very high, better than 99 percent. If an object presents a sufficiently high RCS to the radar, e.g. that of a 1 cm² object, it will be detected and data will be recorded because of the low recording threshold. Furthermore, the nature of the data allows false alarms due to noise to be easily separated from true detections in later processing of the data. Given a detection, the probability of an undetected false alarm is estimated to be 10⁻⁹.

Calibration results indicate that PP RCS can be determined to an accuracy of ± 0.5 dB when the object passes through the central portion of the Σpp beam; i.e. within the half power points of the one way beam pattern (0.05°). From the data itself, one can determine whether an object passes through this portion of the beam. The OP RCS should be nearly as accurate as the PP RCS although complete calibration results are not available. The effects of noise on the measurement of the PP and OP RCS can be mitigated since the contributions of all the pulses received as the object crosses the beam are integrated in the post mission processing.

Orbital parameters are determined with varying degrees of accuracy. The position of the debris object as the data are taken is determined well enough for debris modelling purposes because of the precise range measurement available from the radar and the angle estimates that can be employed to calculate the other two position coordinates. The accuracy of other orbital parameters, here we use orbital inclination and eccentricity, depend on the accuracy of measurement of the three components of the object's velocity. The radar measures one component, the range rate, very accurately but the other two must be calculated by differences in calculated positions determined from successive radar pulses. These positions are derived from angle measurements on individual pulses and are subject to error because of low signal to noise ratio and calibration errors; the differences are especially subject to error. A quantitative discussion of orbital inclination and eccentricity accuracies follows.

Figures 13 and 14 show the results of a calculation which illustrates the situation for a particular case in which the radar beam pointed south at 10° elevation and the debris object is in a 500 km altitude circular orbit at various inclinations. The (small) debris object provides only a 15 dB signal to noise ratio on each pulse at the radar; a 10% calibration error is assumed. Figure 13 shows that the error in inclination estimates varies from about 1.5 to 6 degrees. Figure 14 shows that except for "high inclination" i.e. near-polar orbits (60° to 120°) errors in the eccentricity estimates are quite large. For this case the contribution of the low signal to noise ratio dominates the contribution of calibration error to both the inclination and eccentricity errors. For larger objects (high signal to noise ratio) calibration error would be the dominate error effect.

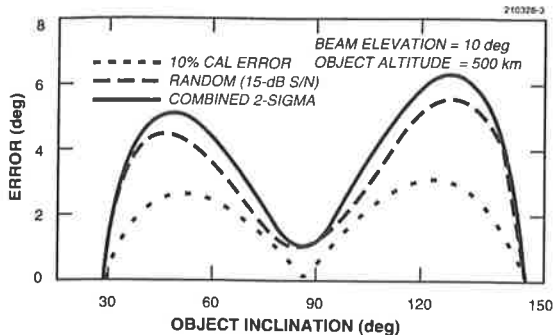


Figure 13. Orbital inclination estimation error.

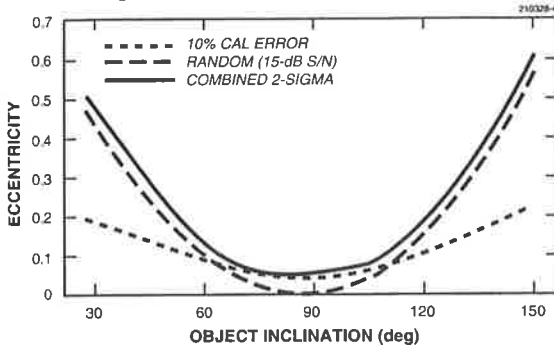


Figure 14. Orbital eccentricity estimation error.

Further results on the estimation of orbital parameters are available from the results of so-called "fly-thru" tests. These tests were used to emulate collection of debris data in a controlled manner with known targets. In these tests, the radar beam was parked ahead and along the orbit of a known resident space object (RSO), and data were gathered as the object passed through the beam. This was very nearly an end-to-end test of the debris mode. Fly-thru tests helped to determine how well the orbital parameters of the objects could be measured and what conditions affected the quality of the data.

The analysis of fly-thru data was conducted as follows:

- Data were reduced to provide pulse by pulse estimates of target returns in the four channels and associated estimates of range, range rates, and beam pointing angles. For each pulse containing a target return, the range-Doppler cell of the target was found. The Σ_{pp} , Σ_{op} , ΔAz , and ΔEL voltages were determined. Calibration constants (i.e., monopulse gradients) were applied to the real parts of the $\Delta Az/\Sigma_{pp}$ and $\Delta EL/\Sigma_{pp}$ ratios to establish the off-axis (monopulse) angles. A weighted (by signal-to-noise) least squares procedure was used to obtain estimates of the target angle rates. Plots of the various quantities were produced.
- Monopulse gradients derived from spiral-scan data were used to estimate the target state vector and resulting orbital parameters. Estimates of inclination and eccentricity were compared to their known values to assess their accuracy.
- Measurements were compared to the best available independent prediction. Estimates of position and velocity (i.e., range, azimuth, elevation, and their rates) were made around the time of each fly-thru based on the catalog. From these data, second derivatives were inferred. It was then possible to numerically adjust the time of validity of each fly-thru to minimize the errors in elevation and azimuth. The result was assumed to be the "true state" of the time of each fly-thru. It was compared to the measurements to see where errors lie.

Results of this analysis were obtained for calibration spheres and other known RSO's.

Figure 15 gives results for fly-thru tests of satellite SSC No. 1361, a calibration sphere with a well-known orbit. The filled symbols are results obtained using the single set of monopulse gradients determined over an entire mission period. The estimates were very accurate. Alternatively, results were obtained using gradients from scans done on the same pass as the fly-thru. The results are shown by the open symbols, and were not as good. This suggested that the variations in the gradient estimates were either not real or produced by noise, and improved with averaging.

Fly-thru tests were performed on other known RSO's. These were typically low altitude objects with high signal-to-noise ratios. In contrast to the spheres, these RSO's tended to have strong OP returns. In this respect, they were similar to the larger debris objects of interest.

Figure 16 shows results for these RSO's; SSC Numbers are given to the right of the figure. Both eccentricity and inclination errors were larger than those for the spheres. One reason for this may be that these objects frequently had strong cross-polarized (OP) returns. In such cases, the monopulse signals were likely to be corrupted by OP signal coupling to the PP angle channels (i.e. the ΔAz and ΔEL channels). Another reason may be that the tracks of these objects were less accurate than those of the spheres. As a result, these objects were less likely to fly through the center of the beam, where monopulse gradients are most accurate.

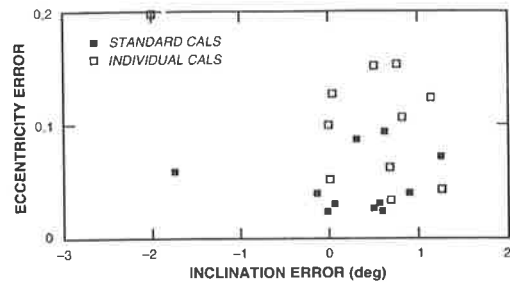


Figure 15. Calibration sphere fly-thru results.

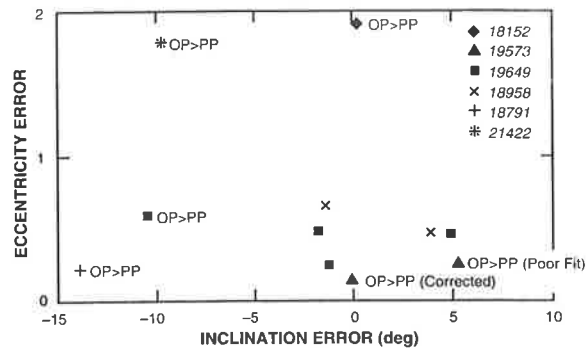


Figure 16. Resident space object fly-thru results.

Cases in which the OP return appeared to exceed the PP return produced larger errors. The case of SSC No. 19573 (triangles) received special attention. As this object passes through the beam, the OP/PP ratio changed. The initial fit to the data was very poor. Slopes were corrected using that portion of the data having lower OP/PP ratio and the estimates were substantially improved. As a result, it appeared that orbital parameter estimates were degraded whenever the OP return exceeded the PP return.

In summary, all the inclination estimates were within 15 degrees of the truth. For targets having OP/PP less than 0 dB the inclination estimates were all within 5 degrees of the truth. From the data itself the OP/PP ratio is available for each debris object detected for use by the users in interpreting that data. Eccentricity estimates appeared useless, even for somewhat favorable conditions. Sphere fly-thru tests gave better results than other RSO fly-thru tests.

Comparisons of the measurements with predictions based on the catalog showed, as expected, that principal sources of error were angle rate estimates derived from the monopulse data. These data are apparently corrupted when the cross-polarized return is high. However, there were cases of favorable OP/PP and favorable crossing geometry for which the monopulse slopes appeared to be in error. While the cause of this was uncertain, a contributing factor may have been an inadequacy in the simple linear calibration used to obtain the monopulse gradient.

To address concerns of linear monopulse calibration, higher order polynomial fits to the monopulse calibration data were employed. Reference 2 provides more details. The linear fit (Figure 17) shows that there was some weak coupling between the two angles. The third order fit results (Figure 18) shows a nonlinearity of the monopulse characteristic that is not surprising for large off-axis angles. Examination of higher order fits indicated that a third order polynomial would be sufficient to represent the monopulse characteristic within the main beam (0.05 degrees). Use of a third order model typically results in an improvement of 1° in inclination estimates relative to the first order model. Spiral scan data is shown superimposed on the third order fit in Figure 18.

7. ORBITAL DEBRIS MEASUREMENT RESULTS.

As indicated in Section 1, a large number measurement hours of Haystack Radar data on orbital debris is available; this number will increase substantially in the next few years. Results and interpretations of these data are being reported by NASA. Some summary results from Reference 3 are discussed here. Figure 19 shows the cumulative detection rate of debris objects, which is proportional to the debris population, as function of object diameter as inferred from the object RCS based on a sample of approximately 800 hours of data. To within the sampling accuracy as indicated by the error bars, the detection rate measured by the Haystack Radar as a function of object size is in agreement with predicted values determined from debris density models.

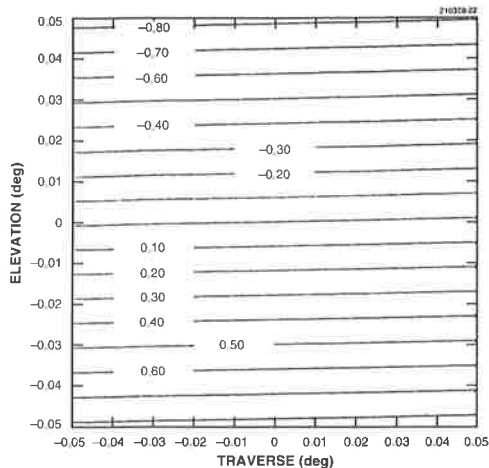


Figure 17. First order elevation monopulse contours.

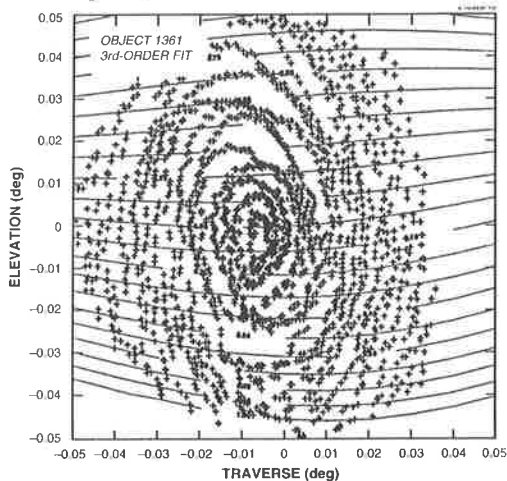


Figure 18. Third order contours with spiral scan data.

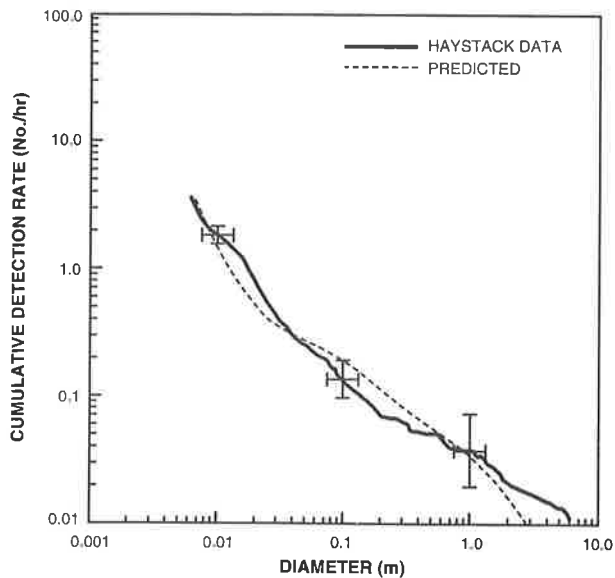


Figure 19. Measured and predicted detection rates vs object size.

Figure 20 shows detection rates versus object altitude for a small sample of 188 hours of data. Comparison of the Haystack data with the predicted curve indicates rough agreement or at least no disagreement with predicted values considering the small sample size. Future results from larger sample size will be of interest in further study of correlation between predicted and measured values. The striking result shown in Figure 20 is the large difference between Haystack detections and the number of detections expected based on the approximately 7000 objects in the catalog. The measurements clearly indicate that the number of (small) debris objects far exceeds the number of cataloged objects.

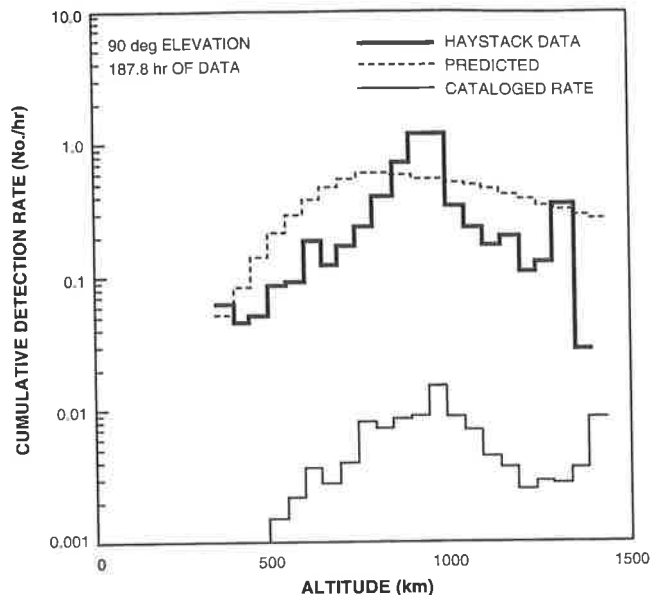


Figure 20. Measured and predicted detection rates and catalog rate vs altitude

8. HAYSTACK AUXILIARY RADAR

This radar will obtain orbital debris data that is complementary to that obtained from the Haystack Radar. Operating at Ku-Band it will be employed at high elevation angles, primarily 90°. Figure 1 also shows the half-completed HAX radome as it was in October 1991. Key parameters are shown in Table III. The Auxiliary Radar shares the processing system of the Haystack Radar so it will have all of the processing and waveform flexibility of Haystack.

Table III

Center Frequency	16 GHz
Antenna Diameter	12m
Beam Width	0.105°
Peak Power	120 Kw
Pulse Repetition Frequency	30-1350 pps

9. SUMMARY

A considerable amount of orbital debris data has been collected (1900 hours) with the Haystack Radar and agreements are in place for collection of much more: 1600 hours per year total from Haystack and the Haystack Auxiliary Radar for several more years. Very careful operation and calibration of the radar systems is required to produce reliable, accurate data.

Low threshold detection and subsequent processing steps to remove false detections provides a better than 99% reliability for detecting orbital debris. Radar cross section measurements, used in subsequent processing to estimate size, mass, and other properties of debris objects, are estimated to be accurate to approximately ± 0.5 dB.

Estimates of orbital parameters of a debris object can have significant errors because of the need to estimate velocity from successive position estimates each obtained from a single radar pulse. Orbital inclination estimates are expected to be within 5° of their true values in many cases. Estimates of eccentricity can be subject to large errors.

10. REFERENCES

1. T. L. Sangiolo and L. B. Spence "PACS: A Processing and Control System for the Haystack Long Range Imaging Radar", *1990 IEEE International Radar Conference*, 90CH-2882-9, 7 May 1990.
2. B. W. Zuerndorfer et. al., "Calibration of the Long Range Imaging Radar", MIT Lincoln Laboratory Project Report PSL-176, 31 December 1992.
3. E. G. Stansbery et. al., "Characterization of the Orbital Debris Environment Using the Haystack Radar", JSC-32213, NASA Johnson Space Center, 24 April 1992.

This work was sponsored by the Department of the Air Force under contract F19628-90-C-0002.